Sust. Build. **6**, 7 (2023)

https://doi.org/10.1051/sbuild/2023008

Topical issue on: Sustainability in the build environment edited by David Goodfield

Sustainable Buildings

Available online at:
www.sustainable-buildings-journal.org

RESEARCH ARTICLE

OPEN ACCESS

Assessment of large-area luminescent solar concentrators as building-integrated geodesic dome panels

Thomas Flynn[1], Subhash Chandra[2,*], Anita Ortega, and Sarah McCormack[1]

[1] Department of Civil, Structural & Environmental Engineering, School of Engineering, Trinity College Dublin, Dublin,Ireland
[2] Department of Geology, School of Natural Science, Trinity College Dublin, Dublin, Ireland

Received: 30 March 2023 / Accepted: 18 August 2023

Abstract. Luminescent solar concentrators (LSCs) ability to concentrate both direct and diffuse solar irradiation exhibits exciting potential as building-integrated photovoltaics (BIPV) in urban environments. As BIPV elements, LSCs are often imagined as semi-transparent solar windows which can be integrated seamlessly into a building's façade and architectural applications as solar harvesting devices. One application explored in this research is a solar geodesic dome panel for an ongoing community greenhouse development in Derry, N-Ireland. A 4V and 2 m diameter geodesic dome were modelled in Revit, and an Insight Solar Analysis model optimised the LSC-geodesic dome and calculated the solar potential. The triangular LSC panel of 875 cm^2 was modelled using raytracing software to obtain efficiency parameters. Subsequently, fabricated using a luminescent acrylic 6T66 waveguide, edge-mounted silicon solar cells and tested outdoors for 29 h. A power conversion efficiency of 0.60% compared to theoretical power conversion efficiency of 1.49% was measured. In the optimum location of the dome, the LSC panel would produce 444.22 Wh and, overall, 74.2 kWh in a year. While this power generation is essential, semi-transparent LSC-geodesic dome panel transmission can downshift solar radiation in the photosynthetically active radiation range, better suited for plant growth and the greenhouse effect.

Keywords: Luminescent solar concentrators / building-integrated photovoltaics / Insight Solar Analysis model / geodesic dome

1 Introduction

Following the 2021 United Nations Climate Change Conference (COP26) in Glasgow, the nations are committed to limiting the rise in global temperatures to 1.5 °C to mitigate the ongoing global warming crisis [1,2]. Moreover, the EU's ambitious target is to reduce greenhouse gas emissions by 7% annually and 80 to 95% by 2050 to meet long-term decarbonization goals, achieve a climate-neutral, and sustainable society [3]. It requires to reduce the CO_2 emission associated with current energy generation by the transition to renewable energy generation technologies, such as solar energy [4]. Solar energy sources have a theoretical potential to meet global energy requirements [5]. It is one of the fastest-growing technology to meet energy demands, through various forms of electricity, heat, and daylighting. Due to decreasing costs, photovoltaic (PV) panels dominate the solar energy market [6]. However, due to their reliance on direct solar radiation, the energy output of these panels can be unreliable in a climate where diffuse solar radiation dominates, like in Ireland, and especially in urban environments. PV integration in the built environment is challenging and same time hugely important to meet the sustainable building's target [7]. There is various approach has been used to enhance the building-integrated photovoltaic (BIPV)integration [8]. One of them is, to boost BIPV efficiency and functionality by solar concentrator optics, and technology is known as concentrated photovoltaic (CPV) [9,10]. One of the CPV technology, luminescent solar concentrators (LSC) are gaining popularity as they can operate efficiently for both direct and diffuse solar radiation, static nature, high acceptance angle [11–13]. LSCs emerging as effective and practical solutions for sustainable built environments [14–16]. Their benefits shifting solar spectrum, transparency control, ease of integration in building facades, envelopes, and windows, choice of colour, aesthetic appeal, and fabricated using low-cost manufacturing techniques such as moulding and casting [17,18]. LSCs are more suitable candidates for BIPV; potential to achieve near zero building, smart windows, transmitted light used for daylighting, and transmission can be tuned to for daylight and

* e-mail: schandra@tcd.ie

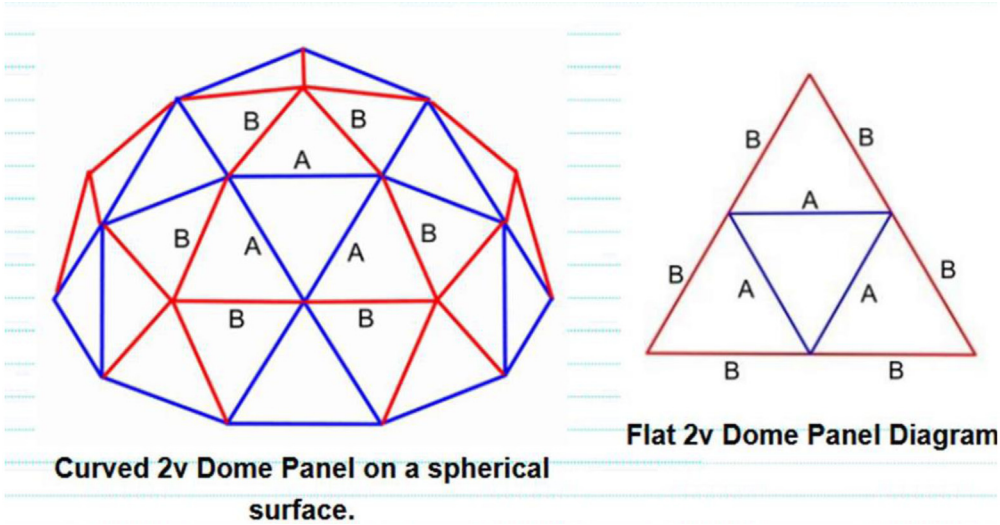

Fig. 1. 2V dome elevation.

photosynthetically active radiation (PAR), collect direct and diffuse solar irradiation help to overcome deploying BIPV in the climate where diffuse solar irradiation is significant such as in Ireland and minimise the impact of shadow in an urban area. Despite lower efficiency compared to semitransparent solar cell, the LSC's are preferred choice for built environment due to ability to shift solar spectrum and operate in diffuse solar radiation. Sustainable built environments, such as geodesic domes, are becoming more widespread in their use as greenhouses, in agriculture, residential, and commercially used spaces [19–22]. They are lightweight, have an aesthetically pleasing design, and have intrinsic solid strength provided by the frame. The freedom of filling the panel allows the LSC integration as a BIPV application. The geodesic domes are dome-like structures with many flat triangular elements. These elements can vary in size, and the number of elements is determined by the so-called frequency of the dome, labelled with the letter V. A two frequency, or 2V dome is shown in Figure 1. Higher frequency means more triangles added to the main panel diagram, meaning more refinement, more elements and smaller element sizes. As the frequency increases, the dome shifts more from an icosahedron shape to a curved dome appearance.

As most of the structural strength in a geodesic dome comes from the frame elements, which are under either tension or compression, the panel infill itself does not face any lateral bending stresses from the self-weight of the structure. As such, the panel is only required to withstand external forces and pressures, such as impact loads, wind loading and snow loading. It gives great freedom in deciding the material to be used in the panel, which ranges from tempered glass to polycarbonate sheeting. This research studied the integration of LSC technology in the geodesic dome as BIPV elements located in Acorn Farm, Derry, N-Ireland. Acorn Farm is an outdoor community development under construction in Derry, in which it is planned to install state-of-the-art renewable energy systems to display. Within the development, there will be a number of geodesic domes used for different purposes, with smaller domes intended to be used as greenhouses and larger domes for exhibition and community spaces. This research has evaluated the power output and efficiency of a triangular large-scale luminescent solar concentrator module integrated within a geodesic dome or similar building-integrated use. Moreover, the aim was to analyse and understand the solar intensity distribution on a geodesic dome structure and fabricate and analyse a triangular LSC panel. It has explored how a semi-transparent LSC panel would operate as a geodesic panel infill in a dome designed to be used as a greenhouse.

2 Methodology

The research methodology used is theoretical modelling and experimental characterisation. Theoretical modelling optimised the LSC-integrated geodesic dome design. Using Revit 2022, the geodesic dome design was modelled. The raytracing model was used to optimise efficiency parameters for triangular LSC geometry as an element of the geodesic dome. The experimental results were obtained from the fabricated and tested triangular LSC panel. Subsequently, the modelling and experimental results were to validate the methodology. The methodology developed in this work used a specific parameter of location, solar irradiation, dome size requirement, solar cell, and LSC as a case study to evaluate the optimisation and performance of LSC integration in the geodesic dome. However, its design is adaptable, expandable, and localised to optimise the LSC-geodesic dome integration and analyse the performance in a given location for different sizes, shapes, and orientations LSC- geodesic dome configurations. Moreover, the methodology can be used for other applications of LSC, such as integration and performance of LSC in building windows and façade. The methodology's uniqueness is that it can estimate the long-term performance of LSC panels integrated with different built environments.

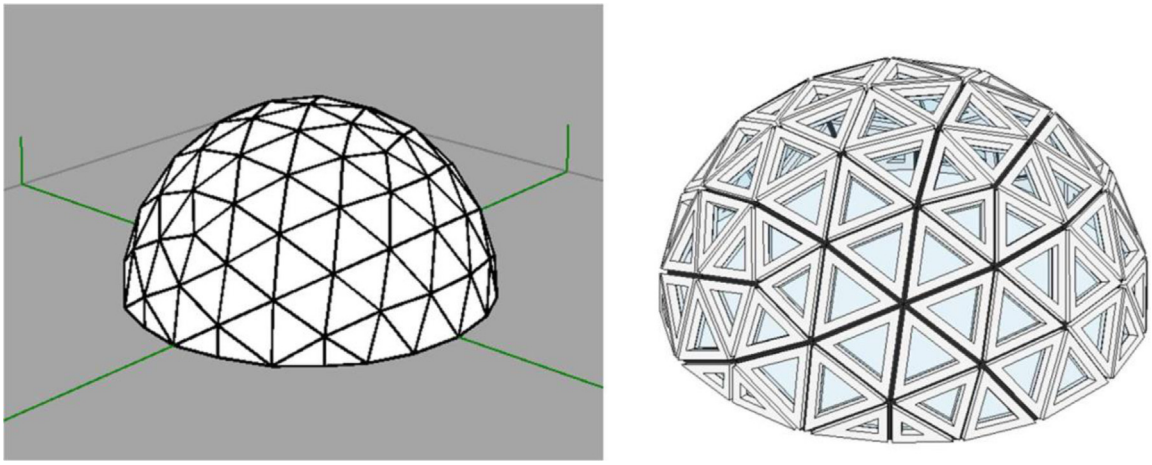

Fig. 2. Geodesic dome model extruded from a regular dome and shown with realistic glazed panel detail of geodesic dome diameter of 2 m.

Fig. 3. Computer generated image of the Acorn Farm site, in which several geodesic dome of 2 m diameter will be built.

2.1 Sun-path solar analysis model

Two theoretical models were created; a toolkit Dynamo visual programming for Revit to design the geodesic dome. It has the functionality to create the geodesic dome panelling, dome frequency, rotation, scale, and adaptive family in Figure 2.

A computer-generated geodesic dome image of the Acorn Farm site was used to estimate the dome diameter and frequency, as shown in Figure 3. The geodesic dome of 4V and 2 m diameter geodesic dome, and its element size was determined using geodesic dome online calculator. The primary element was an isosceles triangle of 59 cm base and 51 cm leg length. It was scaled down to have a base length of 50 cm and leg lengths of 43 cm due to LSC availability of 50 cm^2.

The sun-path model and Insight Solar Analysis for Revit 2022 were used to obtain the solar energy distribution over the geodesic dome for the geographic location in St. Columbs Park House, Derry, N-Ireland.

2.2 LSC ray-tracing model

Pvtrace is an open-source Python-based statistical photon path tracing software developed, by Daniel Farrell, was used for optimizing the LSC element for geodesic dome [23].

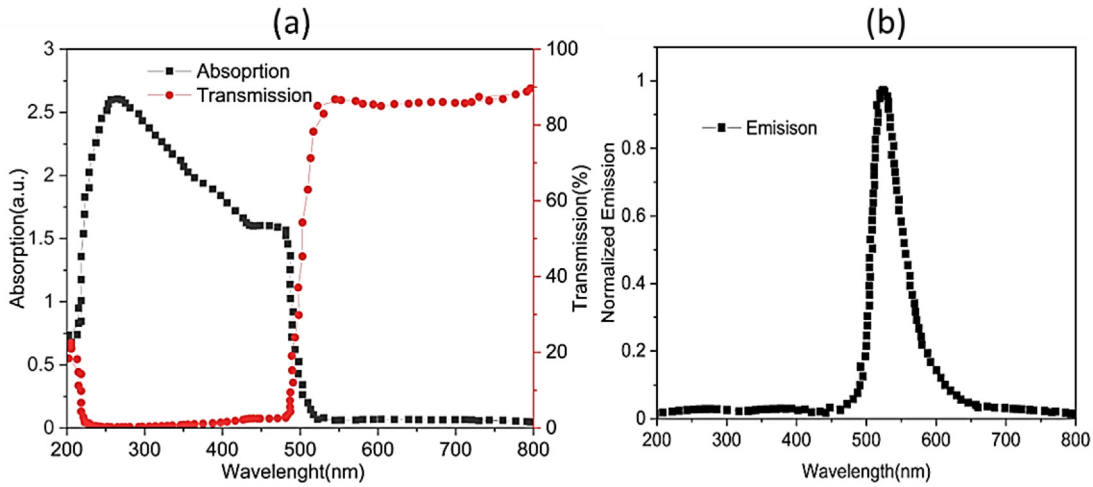

Fig. 4. Luminescent acrylic 6T66 absorption, transmission, and emission spectra were measured experimentally. Absorption range is 200–500 nm, transmission is nearly zero in 200–500 nm and 90% above 500 nm, and the emission range is largely centred between 500 and 650 nm.

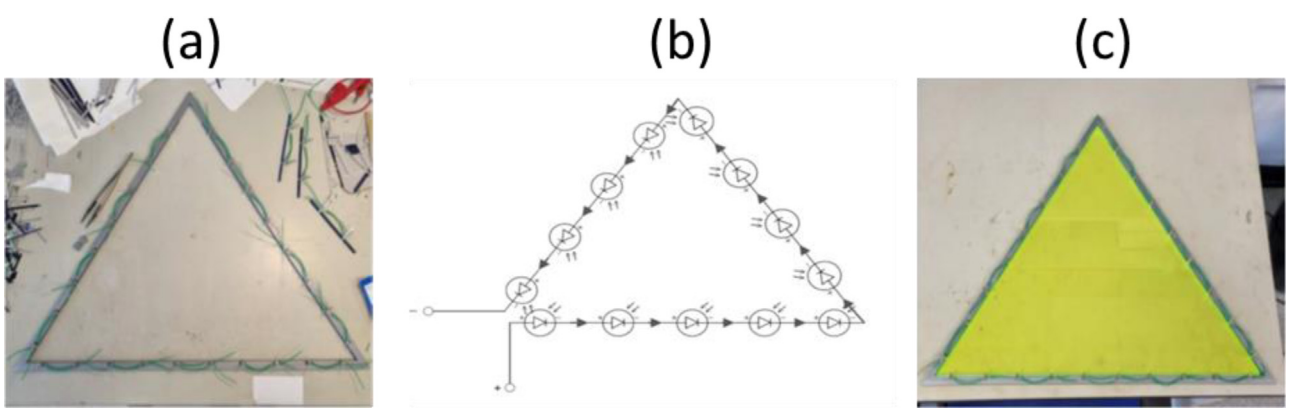

Fig. 5. (a) 3D-printed frame with solar cells, (b) Circuitry diagram of the finalised frame, (c) LSC integrated in 3D printed frame.

Rays are tracked through an object, and their interactions at each boundary recorded until the rays exist or are lost. In that process, the ray goes through various physical processes of reflection, refraction, absorption, emission, scattering, and re-absorption. The model was modified to add the triangular prism geometry in the model code. The input parameters of LSC shape, dimension, and materials used. The materials used are a Luminescent Acrylic 6T66; its absorption and emission spectra are in Figure 4. The input parameter used in for the modelling were a refractive index of 1.5, fluorescence quantum yield of 95%, polymer, absorption coefficient, scattering coefficient, quantum yield, and emission spectrum. Using the model, LSC, optical efficiency and waveguide efficiency were optimized. In addition, the model optimized the optical and power conversion efficiency (PCE).

2.3 Fabrication of dome-LSC element

The prototype of a triangular LSC panel matching the element in the geodesic dome was fabricated. Prusa i3 MK3 3D printer 3D printed Acrylonitrile Butadiene Styrene (ABS) frame used for the geodesic triangular element frame structure, onto which the triangular LSC, solar cells and connection wiring were attached. The frame six arms were printed and glued together as in Figure 5a. The edges were smoothed using fine sandpaper before glueing for better adhesion. The silicon solar cell from DMEGC, with an efficiency of 22%, was used in this study. The standard operating parameters are; Nominal Operating Cell Temperature (NOCT) of 42 ± 3 °C and Temperature Coefficient of −0.330%/ °C. However, due to dome-LSC panel fabrication and electrical connection difficulties, only one

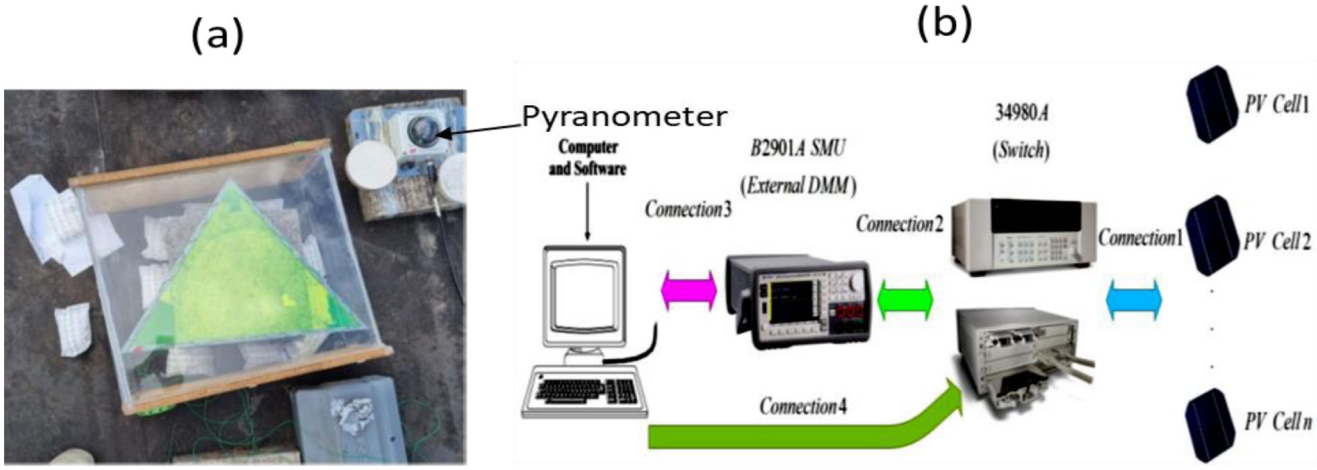

Fig. 6. (a) LSC panel on the roof of the Simon Perry building for outdoor solar analysis, (b) Automated solar cell testing setup.

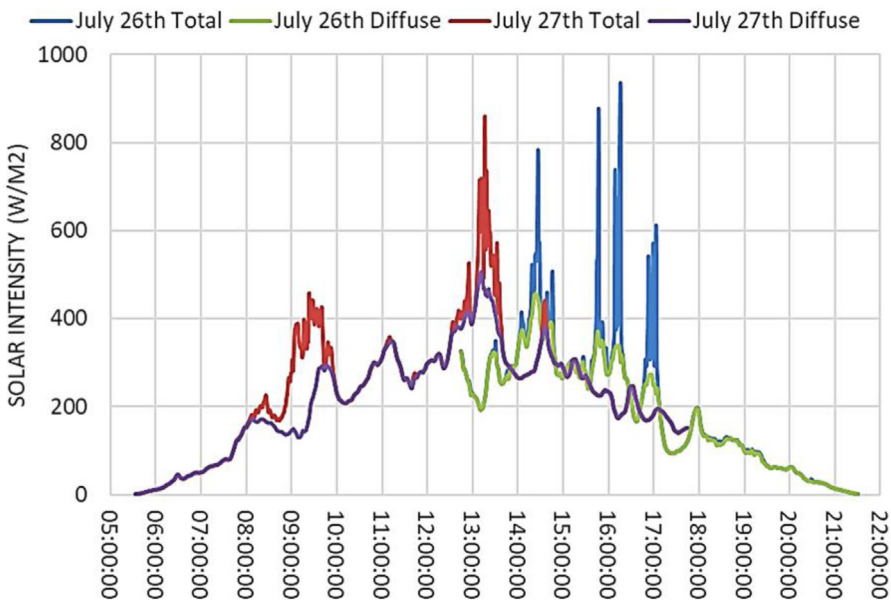

Fig. 7. Solar irradiance distribution between 05:30 and 21:30 on the 26th-27th July 2022.

bus bar from the front and rear of the solar cell was used for electrical connection, which reduced the efficiency to 14%. The solar cells were cut in 100 ×10 mm and 50 ×10 mm by SunWare GmbH. The solar cells were connected in the series and attached to the frame; its circuitry is illustrated in Figure 5b. The voltage was tested to ensure the circuit was operating as expected. The value reached in lab conditions was 4.8V, which equates to an average of 0.37V per cell.

The LSC was placed in the middle of the frame and glued the space between the solar cell and LSC edge to make sure the existing light coupled to the solar cell in Figure 5c. A clear 5 mm thick Perspex panel for the support and SYLGARD 184 Silicone Elastomer encapsulant was used for protection.

2.4 Outdoor testing

The panel was tested in outdoor testing to determine the panel's power output and efficiency. Testing was undertaken on 26th July 2022, on the roof of the Simon Perry, Trinity College Dublin. The testing system is automated with capabilities recording the data with an interval of 1 min in Figure 6b. The power, solar irradiation, and temperature data was recorded. every minute over 29 h.

3 Results and discussion

The outdoor testing data was converted using Visual Studio to calculate the maximum power output (P-max) per minute. PCE of the panel was also calculated. The solar

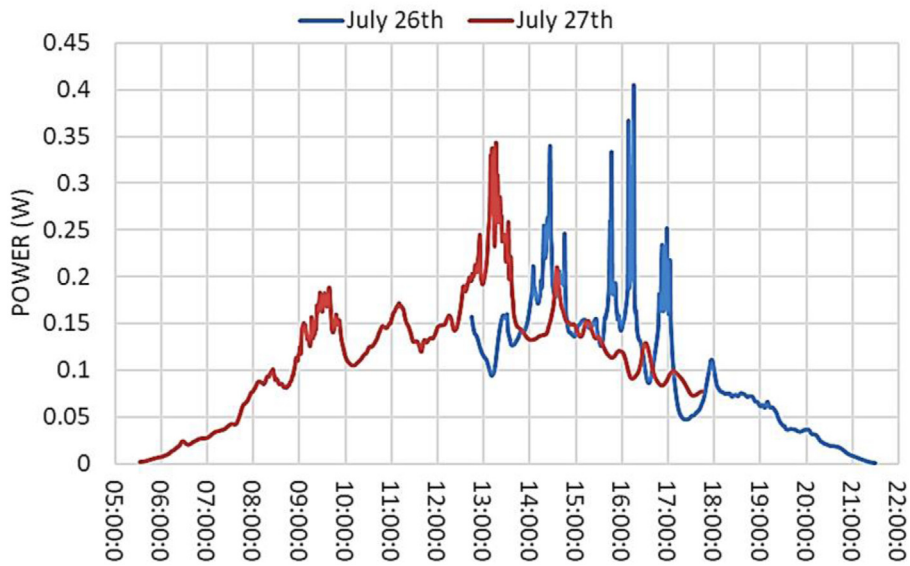

Fig. 8. Maximum power output per minute between 05:30 and 21:30 on the 26th-27th July 2022.

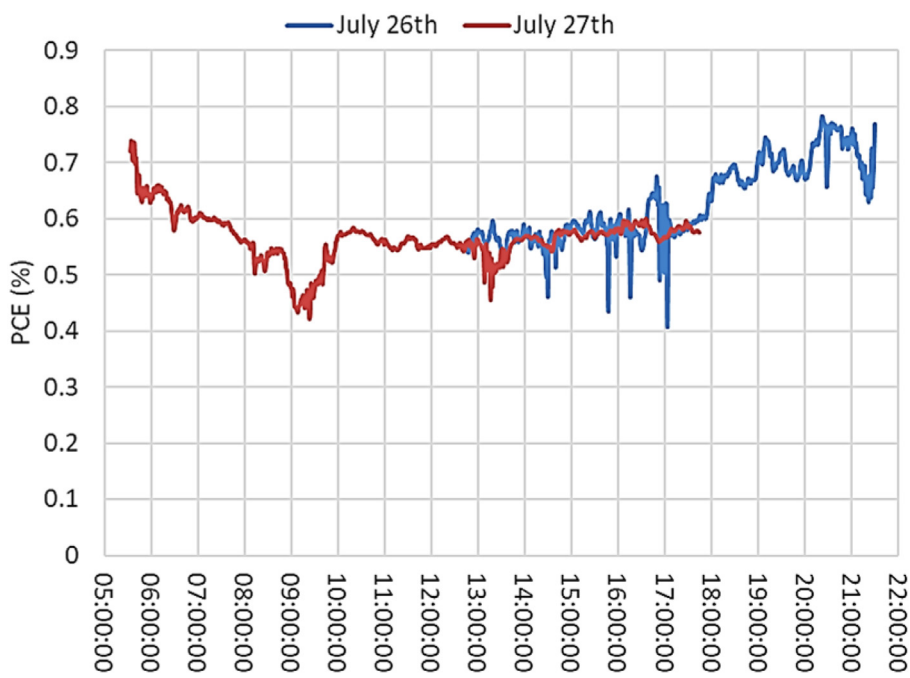

Fig. 9. PCE distribution between 05:30 and 21:30 on the 26th-27th July 2022.

irradiance was measured between 05:30 and 21:30, as this is the time between sunrise and sunset on this date, the total daylight hours, shown in Figure 7.

There were 21 daylight hours, and diffuse irradiation dominated the total solar irradiation. The average total solar irradiance over the twenty-one daytime hours was 222.4 W/m^2. The maximum power in watts taken at minute intervals in shown in Figure 8, and the total energy generated is 2.3 Wh.

PCE of the panel over time is shown in Figure 9, with the average efficiency between sunrise and sunset being 0.60%. The peak power output follows the irradiance; however, unsurprisingly, the PCE is higher around sunrise and sunset, when the diffuse irradiance dominates.

It was observed that air gaps between the LSC edges and solar cell, which prevent 100% coupling of light, added some error in PCE.

Sun-Path Solar Analysis: The Insight Solar Analysis for Revit optimises incident solar energy distribution throughout geodesic dome design. In that, the input of geographical location and sun path settings. In the sun path model, the sun tracks the year between sunrise and sunset using the sun path at the project's designated geographic location, illustrated in Figure 10.

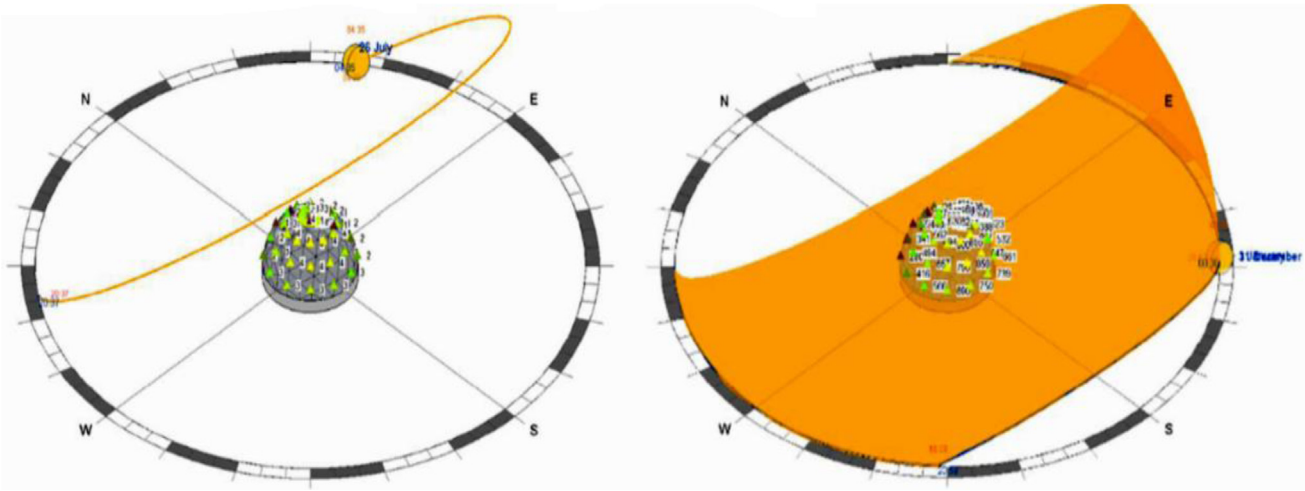

Fig. 10. Illustration of sun path for one day and one year for 2022.

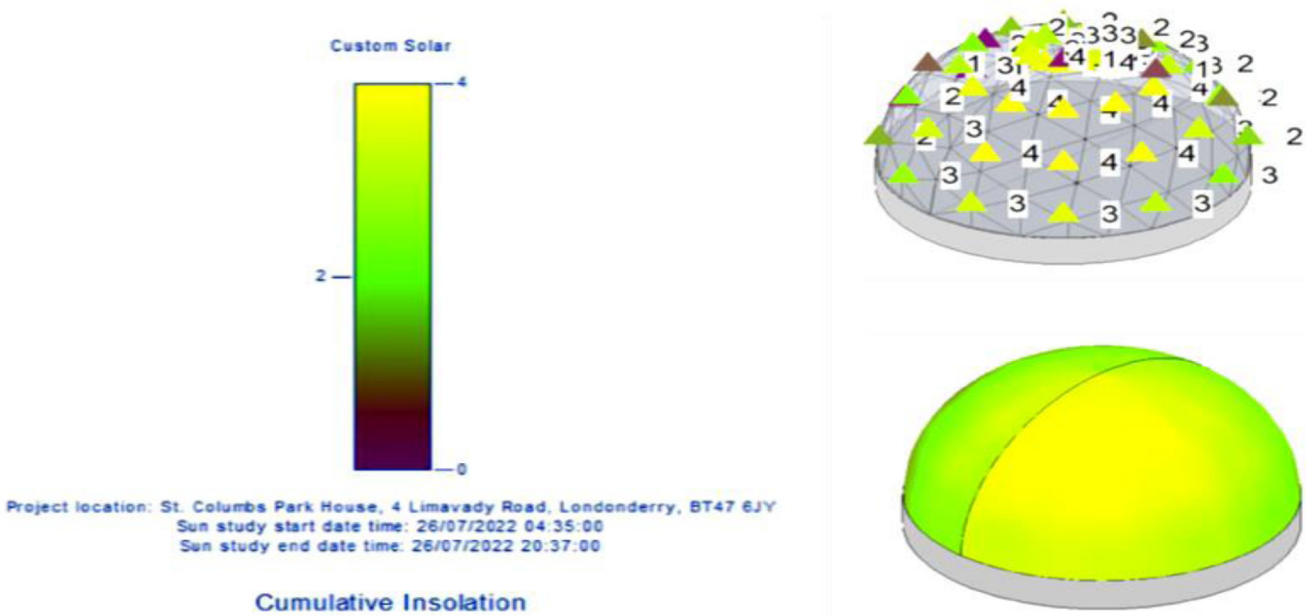

Fig. 11. Solar irradiance distributed over a regular dome and analyzed by points superimposed onto the geodesic dome.

The solar analysis interface allows for the results to be illustrated at specific points in a mesh rather than over the whole surface, superimposed onto the geodesic dome in Figure 11. As the data was collected at 48 analysis points distributed around the dome, the point with the peak solar irradiance could be identified and analyzed to obtain results for the panel with the highest average solar radiation over the period.

The Insight Solar Analysis modelling results are summarized in Table 1. The data between sunrise and sunset for the 26th and 27th of July 2022, in a total of 21 daylight hours, was analyzed, like the experimental. The panel efficiency was always assumed to be the same as the experimental value. The model predicted 204.55W/m^2 average solar irradiance over the geodesic dome location for the 26th and 27th of July 2022, slightly lower than the experimental location, 222.4 W/m^2. The energy generation was 2.255 Wh, marginally lower than the experimental value of 2.3 Wh. The model predicted points with the highest solar irradiance and power output in Table 2.

These comparisons concluded that the experimental and experimental are mainly in agreement. As such, the software can be used to analyse the irradiance over an entire year. The sun settings were changed from 00:00 on January 1st until 23:59 on December 31st, 2022. The data is taken over 4660 daylight hours in the year. Again, the highest average data point was extracted to calculate the yearly results for the panel with the highest average irradiance—the average values over the dome for the year in Table 2.

This model analysis optimized the panel location and performance point over the dome. Figure 12 shows the panels with the highest average over the year (green), the lowest average (red) and the highest peak hour irradiance

Table 1. (a) Average dome output between 26–27th July 2022, (b) Panel with highest average output.

(a)

		Units
Average irradiance	204.55	W/m^2
Total irradiation	4295.6	Wh/m^2
Area	0.0875	m^2
Efficiency	0.6	%
Energy	2.255	Wh

(b)

Optimum panel		Units
Average irradiance	296.345	W/m^2
Total irradiation	6223.25	Wh/m^2
Area	0.0875	m^2
Efficiency	0.6	%
Energy	3.267	Wh

Table 2. (a) Average year dome output for 2022, (b) Panel with highest average output.

(a)

		Units
Average irradiance	117.96	W/m^2
Total irradiation	549676	Wh/m^2
Area	0.0875	m^2
Efficiency	0.6	%
Energy	288.58	Wh

(b)

		Units
Average irradiance	181.57	W/m^2
Total irradiation	846124.8	Wh/m^2
Area	0.0875	m^2
Efficiency	0.6	%
Energy	444.22	Wh

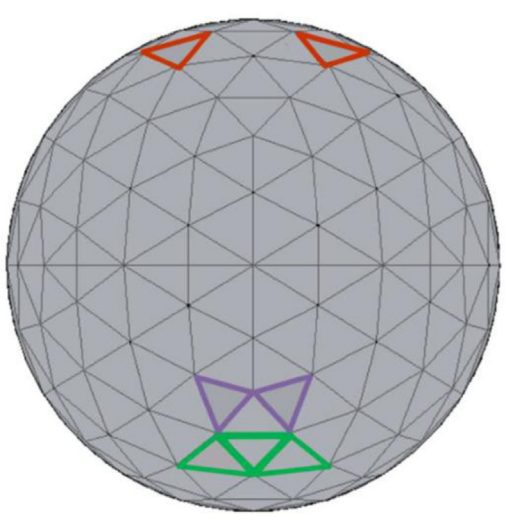

Fig. 12. Plan of dome showing 'green' as highest yearly irradiation, 'red' as lowest yearly irradiation, and 'purple' as highest peak irradiance.

(purple). The highest peak irradiance was 850 W/m^2. This suggests the best and worst candidates for panel locations where only a few LSC panels are to be installed.

The average irradiances regarding the normalized location within the dome were analyzed to assess the effect of panel location. The average irradiance values concerning their relevant positions in the dome were calculated. The coordinates are normalized between −1 and 1, with (−1, −1) South-West and (1, 1) North-East. The points with the highest average irradiance are highlighted in red, as shown in Figure 13, with an average irradiance of roughly 180 W/m^2. The most critical coordinate regarding the yearly average efficiency is the southernmost dimension. The height dimension also has an effect. The analysis point with the highest annual average is located roughly 1.1m (the normalized value multiplied by the radius of 2 m) from ground level and 1.6 m south of the centre point.

The North-South dimension is the most important factor, from an average of 42 W/m^2 at the northernmost point to 170 W/m^2 average at the southernmost in Table 3a. The height is also a contributing factor, with a

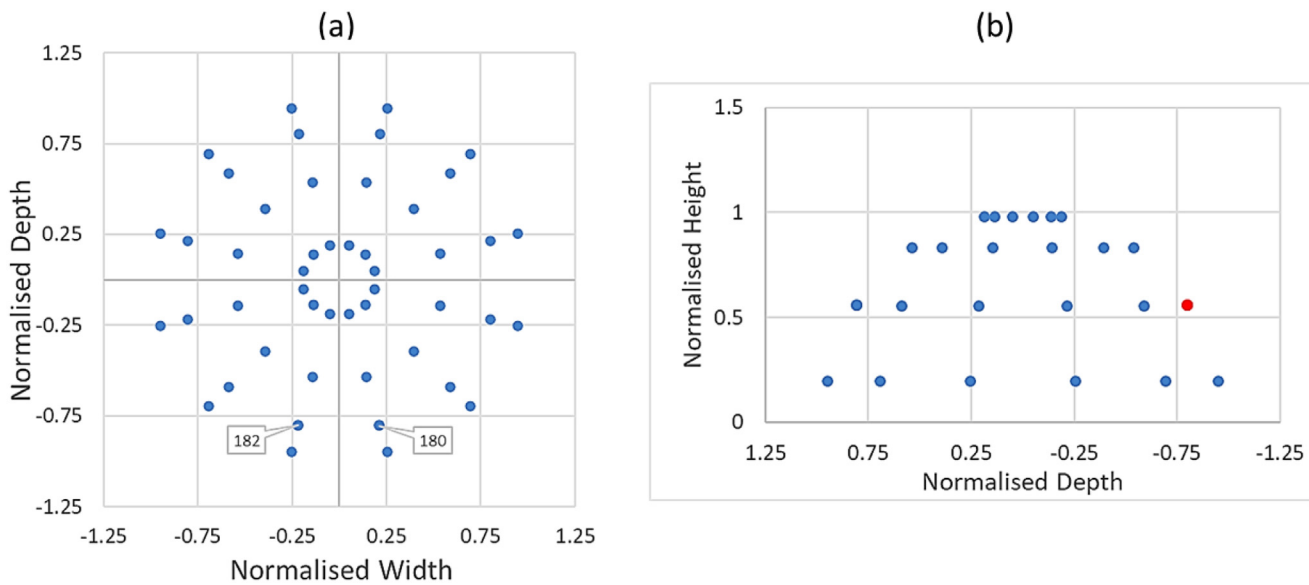

Fig. 13. (a) Plan view of solar analysis points over the dome, (b) West elevation of solar analysis points over the dome.

Table 3. (a) Average irradiance of analysis points from North to South, (b) Average irradiance of analysis points from top to bottom.

(a)

Average Irradiance (W/m^2)	Normalised Depth
41.96	1N to 0.75N
65.4	0.75N to 0.5N
84.93	0.5N to 0.25N
113.12	0.25N to 0
142.02	0 to -0.25S
139.81	-0.25S to -0.5S
161.86	-0.5S to -0.75S
170.03	-0.75S to -1S

(b)

Average Irradiance (W/m^2)	Normalised Height
131.59	0.98
125.38	0.83
115.34	0.55
99.52	0.2

Table 4. (a) Surface counts and panel summary for the main triangular LSC panel, (b) Efficiencies and losses of each panel mode.

(a)

Optical Efficiency (%)	9.9
Waveguide Efficiency (%)	64.3
Thermodynamic Prediction (%)	14.9
Non-radiative Loss (%)	7.5
Geometric Concentration	12.865

(b)

	Triangle	Equal Surface Area Square	Equal Edge Area Square	50cm Edges Square
Optical Efficiency (%)	9.9	12.1	11.2	9.9
Waveguide Efficiency (%)	64.3	64.7	64.0	58.2
Thermodynamic Prediction (%)	14.9	13.2	11.7	8.3
Non-radiative Loss (%)	7.5	6.7	7.4	7.2

Table 5. (a) Percentage of incident rays collected, escaped, or lost. (b) the histogram of incident rays' distribution (green- transmitted, blue-lost luminescence, and orange-collected at the edges).

(a)

	Triangle	Equal Surface Area Square	Equal Edge Area Square	50cm Edges Square
Collected at Edge (%)	9.9	12.1	11.2	9.9
Escaped (%)	82.6	81.2	81.4	82.9
Lost (%)	7.5	6.7	7.4	7.2

(b)

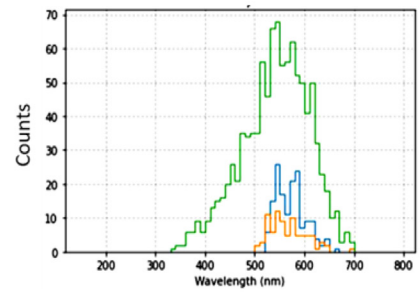

difference of roughly 32 W/m^2 between the top and bottom of the dome in Table 3b. The West-East dimension does not have as much influence, with the dimensions nearing zero having slightly higher values since this dimension coincides with the southernmost and northernmost points.

3.1 LSC ray-tracing

Simulations were run using 1000 rays (each representing a photon) for the LSC panel, and the parameters of LSC are in Table 4. The silicon solar cell with 14% efficiency (two bus connection was used out of four) was used for this work, and the triangular LSC panel optical efficiency of 9.9%, which would equal to PCE of the panel of approximately 1.49%.

Table 5 illustrates the percentage of incident rays which are either transmitted to the edges, escape through the top and bottom surfaces, or are lost along the way. Escaped rays can be rays passing straight through the waveguide unaffected, reflected off the bottom surface and escaping through the top without absorption or re-emitted at longer wavelengths and exited through the top or bottom surfaces. Lost rays are not accounted for in any surface, i.e., lost within the waveguide by processes such as re-absorption. Out of 1000 thousand rays, 771 are not absorbed; transmitted through and reflected from top surface pass. The nearly 50% of rays that pass through that can be used for the daylight, PAR range, and greenhouse effect in a geodesic dome. The 229 rays absorbed, out of that 99 or 43.2%, reach to the edge-mounted PV cells. Therefore, overall optical efficiency of LSC is 9.9%.

4 Conclusions

It is an initial model, and triangular LSC shows promising results as a building-integrated solar geodesic panel and is a solid basis for further research. The sun path model for REVIT is a suitable tool to assess the solar potential of an LSC-integrated geodesic dome in a particular geographical location. The ability to pinpoint the location with the highest available solar irradiance in the model helps to optimise the panel early on by knowing the specific location, solar angle, and size. While the Pvtrace functionality worked very well within this project, validating the results obtained using this model with results from other ray-tracing models could be worthwhile.

The most important parameters to compare are the power outputs and efficiencies. In the obtained triangular LSC panel, the experimental PCE of about 0.60% is comparable to PCEs of other LSC panels of similar sizes and dyes reported in the literature, Zhang et al. reported a PCE of 0.98% for a $31 \times 31 \times 0.3$ cm Red-305/Yellow-083 LSC, and Wilson et al. reported a PCE of 1.55% for a $60 \times 60 \times 0.3$ cm Red-305 LSC [24,25].

The approximated PCE of the triangular panel of 1.28% from pv trace is considerably higher than the 0.60% measured experimentally, likely due to imperfections in the fabrication LSC panel. The solar insight analysis for REVIT 2022 was able to model and predict the LSC-integrated geodesic dome. The energy output for a panel with the dome average solar irradiance over a year would be 288.6 Wh. For the panel with the highest average solar irradiance over the year, the energy output would be 444.2 Wh. This considerable difference between the total dome average and the panel with the highest average highlights the importance of carefully considering the location and angle of the panel to be installed. As shown with the Revit model, the ideal panel is located at a point balancing both the southernmost dimension and the height from ground level.

Assuming a 90:10 distribution of panels to frame around the dome, the total energy produced by a dome covered in these LSC panels can be approximated to be 74.2 kWh in a year, assuming an efficiency of 0.60% for a total panel area of 22.5 m^2. With the improved efficiency of the theoretical model, the energy output could be as high as 184.26 kWh in a year. These figures are for the smallest suggested dome on the Acorn Farm site at a diameter of 2m. For this project, the element with the smallest surface area was chosen and then scaled down to fit within the 50 cm LSC squares available in the lab. With increasing dome frequency comes an increased variation in panel sizes. As such, the panel in the optimum position of the dome regarding solar irradiance could be considerably larger than the panel tested in this project.

PCE is dependent on the LSC properties and solar cell efficiency. The efficiency of large-area LSCs can continue to improve towards commercially viable standards. The LSC efficiency highly functions on shape, size, and dye properties, which can be enhanced using different sizes and dyes with a broader solar spectrum absorption range and higher absorption coefficient. Similarly, higher efficiency solar cells, such as concentrated PV, can help improve the PCE of LSC panels and the LSC-integrated geodesic dome. This study established preliminary results and feasibility of LSC-Integrated geodesic domes. It opened a new area of application of large-area LSCs, making them more viable as commercial solar energy solutions.

This is preliminary research exploring the LSC application for the geodesic dome. Further investigation on the applications and impact on the growth of plants, daylighting, and greenhouse required in the next step. Such as if the LSCs panels are to be installed in the geodesic dome in Acorn Farm, it would be important to complete a lighting analysis to determine how the panel colours would affect the plants growth, daylighting, and greenhouse within the dome. As well as the lighting analysis, the internal temperature would be important to model to determine the effect on the growth patterns of the plants and the efficiencies the transparent LSC- geodesic dome. These are the long-term studies to analyse the impact and benefit of it.

Funding

The authors would like to acknowledge the European Research Council grant PEDAL: (639760), H2020 IDEAS (815271) and support funding from Science Foundation Ireland (SFI) and insights from the PEARL PV COST Action Network.

References

1. COP26, COP26 EXPLAINED, 1−25 (2021)
2. W.J. Ripple, C. Wolf, T.M. Newsome, J.W. Gregg, T.M. Lenton, I. Palomo, J.A.J. Eikelboom, B.E. Law, S. Huq, P.B. Duffy, J. Rockström, World Scientists Warning of a Climate Emergency, Bioscience. **71** 894−898 (2021)
3. European Commission, GREEN PAPER A 2030 framework for climate and energy policies, 2–16 (2013), https://climate.ec.europa.eu/eu-action/climate-strategies-targets/2030-climate-energy-framework_en
4. O. Edenhofer, R.P. Madruga, Y. Sokona, K. Seyboth, P. Matschoss, S. Kadner, T. Zwickel, P. Eickemeier, G. Hansen, S. Schlömer, C. von Stechow, Renewable Energy Sources and Climate Change Mitigation: Special report of the intergovernmental panel on climate change, Cambridge: Cambridge University 333–400 (2011)
5. E. Kabir, P. Kumar, S. Kumar, A.A. Adelodun, K.H. Kim, Solar energy: Potential and future prospects, Renew. Sustain. Energy Rev. **82** 894–900 (2018)
6. IEA, Renewables 2022, Analysis forecast 2027, 1–159 (2022)
7. D.J. Sailor, J. Anand, R.R. King, Photovoltaics in the built environment: A critical review, Energy Build. **253** 111479 (2021)
8. B. Norton, P.C. Eames, T.K. Mallick, M.J. Huang, S.J. Mccormack, J.D. Mondol, Y.G. Yohanis, Enhancing the performance of building integrated photovoltaics, Sol. Energy. **85** 1629–1664 (2011)
9. K. Shanks, S. Senthilarasu, T.K. Mallick, Optics for concentrating photovoltaics: Trends, limits and opportunities for materials and design, Renew. Sustain. Energy Rev. **60** 394–407 (2016)
10. Y. Wu, K. Connelly, Y. Liu, X. Gu, Y. Gao, G.Z. Chen, Smart solar concentrators for building integrated photovoltaic façades, Sol. Energy. **133**, 111–118 (2016)
11. S. Chandra, M. Rafiee, J. Doran, S.J. Mc Cormack, Absorption coefficient dependent non-linear properties of thin film luminescent solar concentrators, Sol. Energy Mater. Sol. Cells. **182** 331–338 (2018)
12. M. Rafiee, S. Chandra, H. Ahmed, S.J. McCormack, An overview of various configurations of Luminescent Solar Concentrators for photovoltaic applications, Opt. Mater. **91** 212–227 (2019)
13. A. Goetzberger, W. Greube, Solar energy conversion with fluorescent collectors, Appl. Phys. **14** 123–139 (1977)
14. M. Vasiliev, K. Alameh, M. Nur-E-Alam, Spectrally-Selective Energy-Harvesting Solar Windows for Public Infrastructure Applications, Appl. Sci. **8**, 1–15 (2018)
15. N. Aste, M. Buzzetti, C. Del Pero, R. Fusco, F. Leonforte, D. Testa, J. Triggering a large scale luminescent solar concentrators market: The smart window project, J. Clean. Prod. **219** 35–45219 (2019)
16. M.G. Debije, P.P.C. Verbunt, Adv. Solar Concentrators: Thirty Years of Luminescent Solar Concentrator Research: Solar Energy for the Built Environment, Energy Mater. **2** 12–35 (2012)
17. S. Chandra, J. Doran, S.J. McCormack, M. Kennedy, A.J. Chatten, Enhanced quantum dot emission for luminescent solar concentrators using plasmonic interaction, Sol. Energy Mater. Sol. Cells. **98** 385–390 (2012)
18. Y. Zhao, R.R. Lunt, Transparent Luminescent Solar Concentrators for Large-Area Solar Windows Enabled by Massive Stokes-Shift Nanocluster Phosphors, Adv. Energy Mater. **3 1143–1148** (2013)
19. A. Kolpakov, O. Dolgov, V. Korolskiy, S. Popov, V. Anchutin, V. Zykov, Analysis of Structural Layouts of Geodesic Dome Structures with Bar Filler Considering Air Transportation, Buildings. **12** 242 (2022)
20. W. Gythiel, C. Mommeyer, T. Raymaekers, M. Schevenels, A Comparative Study of the Structural Performance of Different Types of Reticulated Dome Subjected to Distributed Loads, Front. Built Environ. **6** 1–6 (2020)
21. M.K. Vrontissi, Proceedings of the 50th IASS Symposium: Evolution and Trends in Design, Analysis and Construction of Shell and Spatial Structures, Valencia, 1379 (2009)
22. W. Bober, Geodesic domes in built environments, In: Charytonowicz, J. (eds) Advances in Human Factors in Architecture, Sustainable Urban Planning and Infrastructure, Advances in Intelligent Systems and Computing, Springer, Cham. 1214, 105–111 (2020)
23. Pvtrace, (2022). Https://Github.Com/Danieljfarrell/Pvtrace.

24. J. Zhang, M. Wang, Y. Zhang, H. He, W. Xie, M. Yang, J. Ding, J. Bao, S. Sun, C. Gao, Optimization of large-size glass laminated luminescent solar concentrators, Sol. Energy. **117**260–267 (2015)

25. L.R. Wilson, E. Klampaftis, B.S. Richards, Enhancement of Power Output from a Large-Area Luminescent Solar Concentrator With 4.8× Concentration via Solar Cell Current Matching, IEEE J. Photovoltaics. **7**, 802–809 (2017)

Cite this article as: T. Flynn, S. Chandra, A. Ortega and S. McCormack: Assessment of large-area luminescent solar concentrators as building-integrated geodesic dome panels. Sust. Build. **6**, 7 (2023).